

Communication

Qualifying the Role of Indium in the Multiple-Filled $\text{Ce}_{0.1}\text{In}_x\text{Yb}_{0.2}\text{Co}_4\text{Sb}_{12}$ Skutterudite

Jennifer Graff^{1,*}, Jian He^{2,†} and Terry M. Tritt^{1,2,†,*}

¹ 118 Kinard Laboratory, Materials Science and Engineering Department, Clemson University, Clemson, SC 29634, USA

² 118 Kinard Laboratory, Physics and Astronomy Department, Clemson University, Clemson, SC 29634, USA; E-Mail: jianhe@clemson.edu

† These authors contributed equally to this work.

* Authors to whom correspondence should be addressed; E-Mails: jwhubba@g.clemson.edu (J.G.); ttritt@clemson.edu (T.M.T.); Tel.: +1-864-656-5319 (J.G. & T.M.T.); Fax: +1-864-656-0805 (J.G. & T.M.T.).

Received: 13 February 2014; in revised form: 8 April 2014 / Accepted: 14 April 2014 /

Published: 29 April 2014

Abstract: Literature confirms an improvement in the overall TE properties due to the *in situ* InSb nano-dispersed phases located along the grain boundaries in several double-filled $\text{In}_x\text{Y}_z\text{Co}_4\text{Sb}_{12}$ skutterudites. However, the single-filled $\text{In}_x\text{Co}_4\text{Sb}_{12}$ reports contribute enhancement in TE properties solely on the nature of In as a void filler. To qualify the effect of In on the TE properties on multiple-filled skutterudites several multiple-filled $\text{Ce}_{0.1}\text{In}_x\text{Yb}_{0.2}\text{Co}_4\text{Sb}_{12}$ skutterudite samples, with nominal composition $\text{Ce}_{0.1}\text{In}_y\text{Yb}_{0.2}\text{Co}_4\text{Sb}_{12}$ ($0 \leq y \leq 0.2$), were synthesized. A double-filled base-line sample $\text{Ce}_{0.1}\text{Yb}_{0.2}\text{Co}_4\text{Sb}_{12}$ was also synthesized and characterized to create a much fuller depiction of the nature of In and its impact on the TE properties of the filled $\text{Co}_4\text{Sb}_{12}$ -based skutterudite materials. Our results confirm that small amounts of In can be effective at increasing electrical conductivity in the multiple-filled $\text{Ce}_{0.1}\text{In}_y\text{Yb}_{0.2}\text{Co}_4\text{Sb}_{12}$ skutterudite. An increased mobility and thus electrical conductivity result in a 15% increase in the dimensionless Figure of Merit, ZT , in the nominal sample composition, $\text{Ce}_{0.1}\text{In}_{0.05}\text{Yb}_{0.2}\text{Co}_4\text{Sb}_{12}$, which exhibits a state of the art $ZT > 1.4$ at $T = 820$ K.

Keywords: thermoelectric; thermopower; electrical conductivity; multiple-filled skutterudites

1. Introduction

Binary skutterudites, such as CoSb_3 , naturally form a covalently bonded structure, with low coordination numbers, possessing some of the fundamental conditions in favor of a high performance thermoelectric (TE) material; such as, a large unit cell, heavy constituent atomic masses, low electronegativity differences between the metallic and pnictogen atoms, and naturally occurring large carrier mobility values [1]. The general formula for the cubic unit cell is $\kappa_2\text{M}_8\text{X}_{24}$, which is typically written in its simplest form as MX_3 [2]

The skutterudites novel Phonon Glass Electron Crystal (PGEC) structure allows for optimization of thermal and/or electrical properties of these systems. A PGEC material candidate is a compound structure which resembles a system that simultaneously behaves as phonon glass and an electron single crystal, meaning the material should have a short phonon mean free path and a long electron mean free path. Phonon glasses have a very high degree of scattering, where electron crystals have a very low degree of scattering, thus the PGEC material would be best optimized by minimizing thermal conductivity (κ) while maximizing electrical conductivity (σ) [3–9]. This type of “designer materials approach” or “tuning” of the electrical and thermal properties lend themselves well to the approach of maximizing the TE properties of the material. A material’s thermoelectric properties are measured via the Dimensionless Figure of Merit, ZT :

$$ZT = \frac{\alpha^2 \sigma}{\kappa} T \quad (1)$$

where α is the thermopower or Seebeck coefficient, σ is the electrical conductivity, and κ is the total thermal conductivity. The skutterudites’ periodic cubic crystal lattice allows electrons to move more freely approaching the characteristics of an electron crystal. In addition, the large void spaces (or empty cages) can accommodate relatively large foreign elements, which have been reported many times to dramatically lower the thermal conduction through anharmonic vibrations within the material depending on the specific “filler” element chosen to fill the empty cages [10]. These vibrations are reported to reduce heat conduction in the material to values and temperature dependence that is nearly characteristic of glasses [11–19].

Originally, In was introduced into these antimonide based skutterudites as an interstitial doping element which would enter the empty Co cages, as reported by He *et al* [20]. In, in the single-filled $\text{In}_x\text{Co}_4\text{Sb}_{12}$ skutterudite, is successfully observed solely as a void filler via synchrotron X-ray powder diffraction. However, the role of In as a dual filler, as assumed in the previously reported double-filled $\text{Yb}_x\text{In}_y\text{Co}_4\text{Sb}_{12}$, is not well understood. Peng *et al.* report an enhanced σ and a decreased κ as the In content increases in the double filled $\text{Yb}_{0.2}\text{In}_y\text{Co}_4\text{Sb}_{12}$ [15,21]. In the study herein, multi-filled $\text{Ce}_{0.1}\text{In}_y\text{Yb}_{0.2}\text{Co}_4\text{Sb}_{12}$ ($0 \leq y \leq 0.2$) samples were synthesized and compared to double-filled $\text{Ce}_{0.1}\text{Yb}_{0.2}\text{Co}_4\text{Sb}_{12}$ in order to gain further understanding of the nature and role of In in a multi-filled skutterudite system. As multiple heavy elements are introduced into the $\text{Co}_4\text{Sb}_{12}$ skutterudite, a deviation in location and behavior of In is observed as compared to that of the reported single-filled

and double-filled systems. In the present study, In, as well as Yb, have formed *in situ* secondary InSb and Yb₂O₃ nanophases which are visibly distributed along the grain boundaries. The presence of the InSb nanophases, also reported in Li *et al.* [22], positively affect the TE performance of the material. However, a more unconventional synthesis and preparation method was used herein which is much more simplistic than the Li *et al.* method; yet, exudes similar nanostructure results with a favorable influence on the electronic behavior of the skutterudite.

2. Results and Discussion

X-ray patterns clearly show the presence of InSb and Yb₂O₃ secondary phases (Figure 1a,b). SEM images confirm the presence of nanophases migrating toward the grain boundaries (Figure 2). Quantitative energy dispersive X-ray spectroscopy (EDS) results also verify the presence of InSb and Yb₂O₃ nanophases. The DSC curve (Figure 3) validates the presence of the secondary InSb phase revealing an endothermic peak present at ≈ 490 °C. The melting temperature of bulk InSb is 527 °C; however, melting point depression is most likely observed in these samples due to the encapsulation of the InSb within the structure. Because nanoparticles have a much greater surface to volume ratio than bulk materials, they also have reduced cohesive energies, or bonds with neighbors, as seen in the Lennard-Jones potential [23]. Also, according to Lindemann's criterion, the cohesive energy of a material is proportional to the melting temperature [24]. Therefore, depending on the size of the nanoparticle, it is concluded that atoms on or near the surface require less energy to melt and thus melt at lower temperatures than the bulk material [25]. The melting point of Yb₂O₃ (≈ 2355 °C) is nearly 5 times greater than that of the observed endothermic peak in the DSC curve; therefore Yb₂O₃ is stable where the peak occurs. Like the double filled system in Li *et al.* [22], the presence of In as a secondary InSb phase has an effect on the thermoelectric properties of the multiple filled system.

Figure 1. X-ray powder diffraction of the Ce_{0.1}In_yYb_{0.2}Co₄Sb₁₂ skutterudite revealing the presence of minor amounts of (a) InSb and (b) Yb₂O₃.

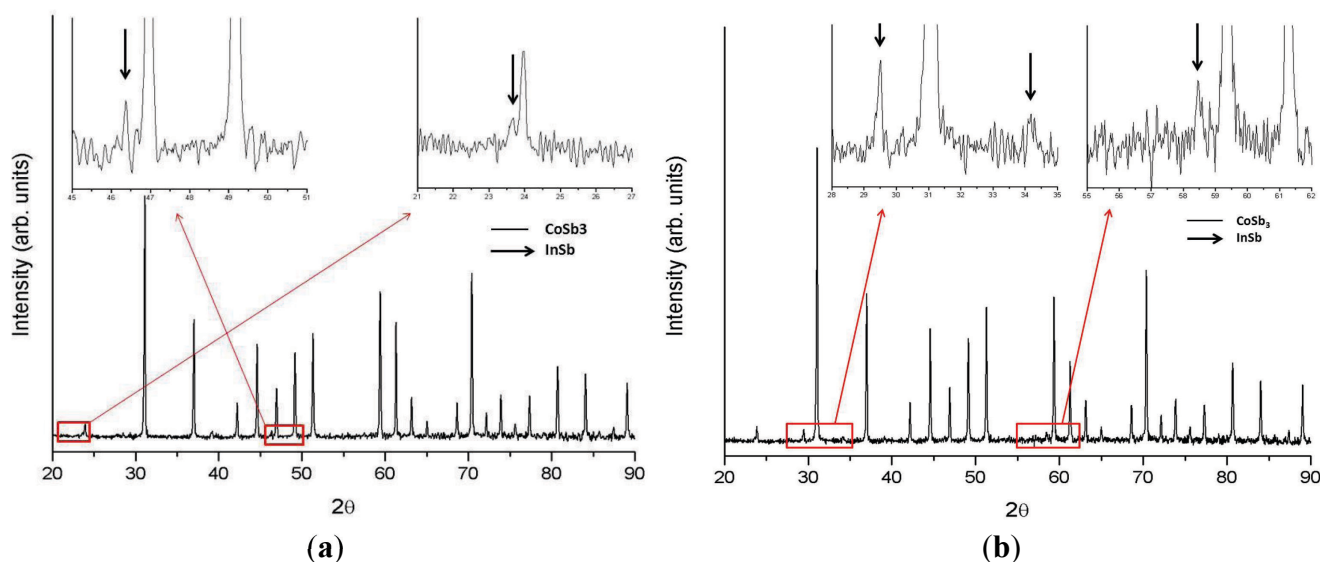


Figure 2. Confirmation of nano-sized secondary phases migrating along the grain boundaries.

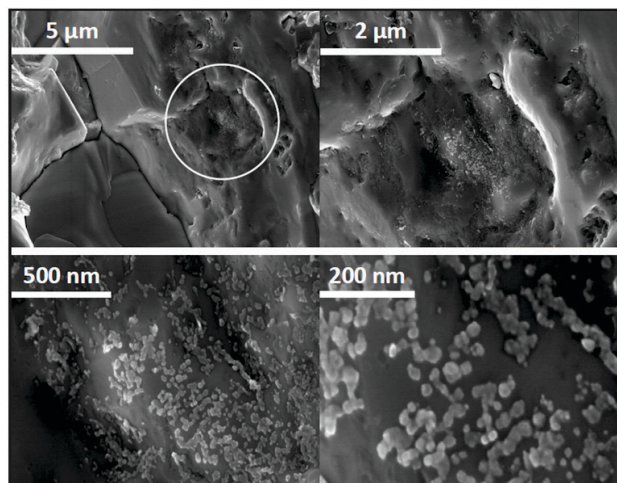
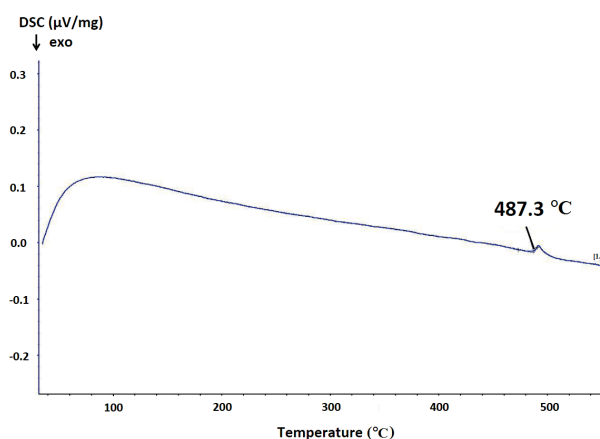


Figure 3. Temperature dependent DSC ($\mu\text{V}/\text{mg}$) revealing a peak at $\approx 490^\circ\text{C}$ further signifying the presence of InSb.



Temperature dependent thermopower (α) and electrical conductivity (σ) are shown in Figures 4 and 5, respectively. Upon observing the thermopower or Seebeck plot, it is evident that an initial addition, $y = 0.05$, of the third filler, In, increases the α by $-10 \mu\text{V}/\text{K}$, this increase in α is confirmed by the decrease in carrier concentration, n , which is observed in Figure 6. However, only small amounts of In addition positively affect the α . As more In is added to the multi-filled skutterudite the α decreases to nearly the same value as the double-filled $\text{Ce}_{0.1}\text{Yb}_{0.2}\text{Co}_4\text{Sb}_{12}$ material. The σ also increases with initial increase of In concentration with a limit on electrical conductivity improvement between $y = 0.1$ and $y = 0.2$. The initial increase in σ is reflected by an increase in mobility of carriers, μ (Figure 7). Small additions of In as a third filler increase both the α and the σ compared to the double filled $\text{Ce}_{0.1}\text{Yb}_{0.2}\text{Co}_4\text{Sb}_{12}$ sample. Total thermal conductivity, κ , is unchanging as the third filler of In is added to the double filled $\text{Ce}_{0.1}\text{Yb}_{0.2}\text{Co}_4\text{Sb}_{12}$ (Figure 8). Additional In does not affect the κ of the material. Therefore, as the κ of the multi-filled $\text{Ce}_{0.1}\text{In}_y\text{Yb}_{0.2}\text{Co}_4\text{Sb}_{12}$ is invariable, the σ and α increase with small additions of In, with a limit to thermoelectric improvement between In amounts of $y = 0.1$ and $y = 0.2$. Overall the multiple filling effect ultimately enhances the ZT as compared to the double filled skutterudite by approximately 15%. The ZT , as shown in Figure 9, is enhanced due to multiple filling

as well as an increase in ZT over the entire temperature range $300\text{ K} > T > 850\text{ K}$ with a maximum $ZT > 1.4$ at $\approx 820\text{ K}$ in sample $\text{Ce}_{0.1}\text{In}_{0.05}\text{Yb}_{0.2}\text{Co}_4\text{Sb}_{12}$.

Figure 4. Temperature dependent thermopower (Seebeck coefficient) of the $\text{Ce}_{0.1}\text{In}_y\text{Yb}_{0.2}\text{Co}_4\text{Sb}_{12}$ skutterudites with the greatest enhancement with $y = 0.05$ In addition.

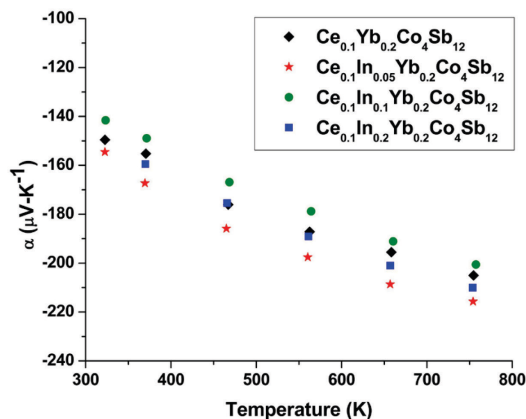


Figure 5. Temperature dependent electrical conductivity of the $\text{Ce}_{0.1}\text{In}_y\text{Yb}_{0.2}\text{Co}_4\text{Sb}_{12}$ skutterudites showing improvement with small additions of In.

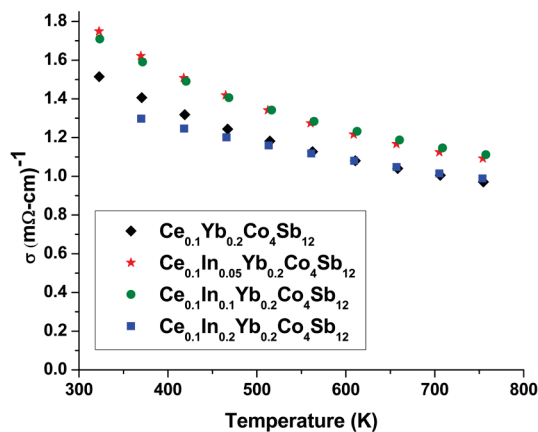


Figure 6. Temperature dependent carrier concentration of the $\text{Ce}_{0.1}\text{In}_y\text{Yb}_{0.2}\text{Co}_4\text{Sb}_{12}$ skutterudites confirming the improvement in thermopower.

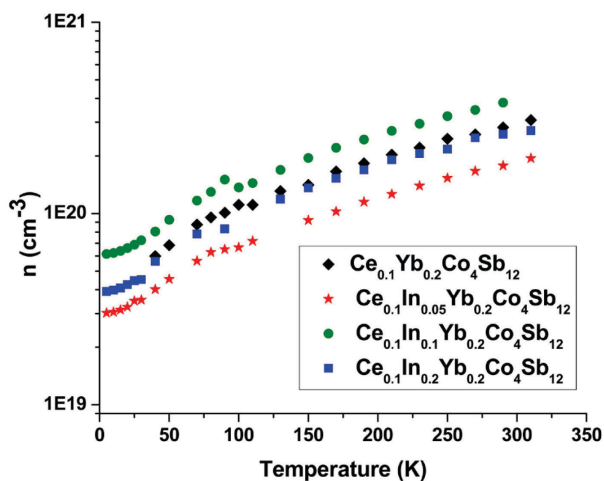


Figure 7. Temperature dependent carrier mobility of the $\text{Ce}_{0.1}\text{In}_y\text{Yb}_{0.2}\text{Co}_4\text{Sb}_{12}$ skutterudites with $\text{Ce}_{0.1}\text{In}_{0.05}\text{Yb}_{0.2}\text{Co}_4\text{Sb}_{12}$ having the most enhanced mobility and thus higher electrical conductivity.

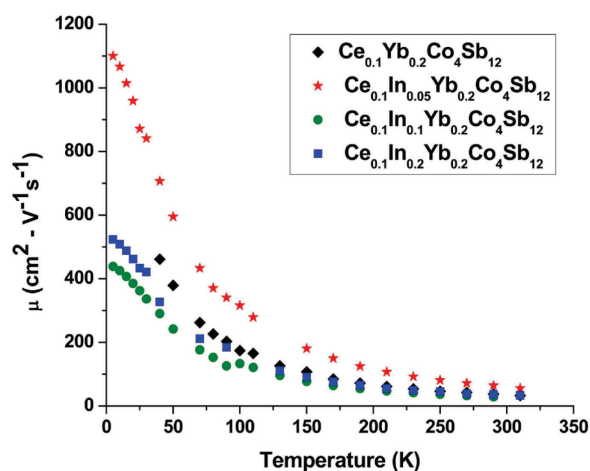


Figure 8. Temperature dependent thermal conductivity of the $\text{Ce}_{0.1}\text{In}_y\text{Yb}_{0.2}\text{Co}_4\text{Sb}_{12}$ skutterudites.

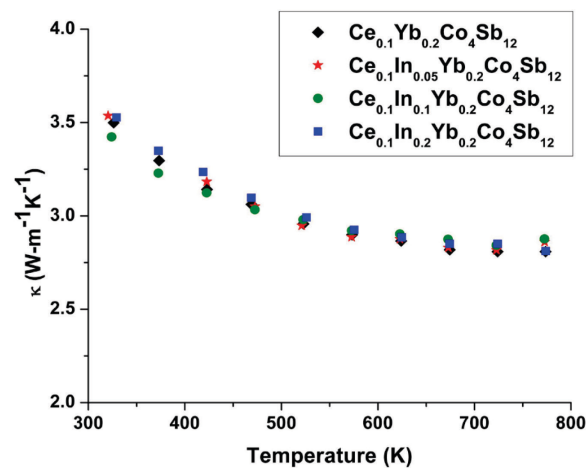
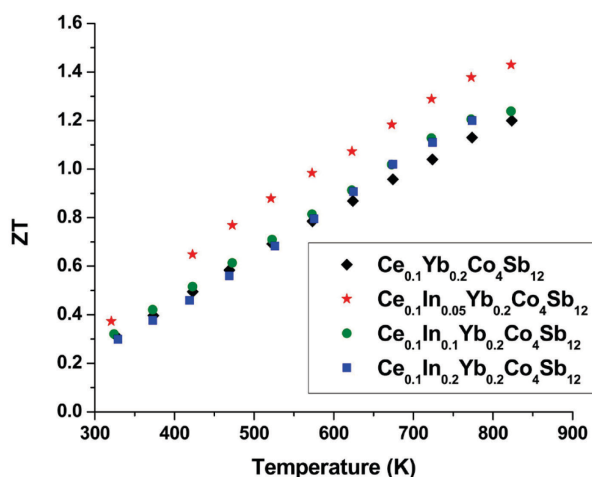


Figure 9. Temperature dependent ZT of the $\text{Ce}_{0.1}\text{In}_y\text{Yb}_{0.2}\text{Co}_4\text{Sb}_{12}$ skutterudites with an overall 15% improvement in ZT for sample $\text{Ce}_{0.1}\text{In}_{0.05}\text{Yb}_{0.2}\text{Co}_4\text{Sb}_{12}$ resulting in a $ZT > 1.4$.



3. Experimental Section

The high purity elements Co powder (99.998% Alfa Aesar, Ward Hill, MA, USA), Sb shot (99.9999% Alfa Aesar), Yb powder (99.9% Alfa Aesar), In ingot (99.99% Alfa Aesar), and Ce powder (99.99 Alfa Aesar) were prepared by mixing, evacuating, and sealing stoichiometric amounts in a quartz tube. The quartz was heated in a Carbolite furnace with the same program previously reported [15]. It is important to note here that no quenching, cleaning, or removal from the furnace, for any reason, of the quartz, was performed during the allotted program. The quartz tubes and resulting ingots were removed from the furnace after completion of the temperature program. The resulting ingots were pulverized using a mortar and pestle, and examined by powder X-ray diffractometry (XRD) using a Rigaku Miniflex® (The Woodlands, TX, USA) diffractometer with Cu K α radiation. The pulverized powders were then made into pellet form (15 mm diameter and \approx 3 mm thick) using a spark plasma sintering (SPS) technique (Dr. Sinter®: SPS-515S; Fuji Electronic Industrial Co. Ltd, Kanagawa, Japan) at 873 K for 15 min. The pellets were then tested for their densities (ρ_D) using dimensional analysis, for their thermal conductivity (κ) by measurements of the thermal diffusivity (D) using a Netzsch Microflash® (Selb, Germany) 457 transient technique, and for heat capacity (C_p) using Netzsch Pegasus® (Selb, Germany) Differential Scanning Calorimeter (DSC) 404. All of these measurements and calculations were used to compute thermal conductivity through the equation $\kappa_T = \rho_D C_p D$. The pellets were then cut into samples that were appropriately suited for measurement of their high and low temperature TE properties, carrier concentration/mobility, and microscopy analysis. High temperature electrical resistivity ($\rho = 1/\sigma$) and Seebeck coefficient (α) values were performed on an Ulvac-Riko (Kanagawa, Japan) ZEM-2 (300–800 K). Low temperature resistivity, Seebeck coefficient, and thermal conductivity were measured within temperature ranges of 6–300 K using a custom design four-probe measurement system [26] for resistivity and Seebeck coefficient measurements and a custom designed steady state system for thermal conductivity measurements [27]. Carrier concentration (n) and carrier mobility (μ) were measured by a Quantum Design® PPMS (San Diego, USA) using the van der Pauw method with the magnetic field strength of $B \approx 0.5$ T (5–300 K). Scanning Electron Microscopy was performed using the fractured bulk samples and sieved powders on an FE-SEM: Hitachi S4800 in order to gain a fuller understanding if micro-morphology and topology of the samples correlate to the observed TE properties as well as confirming the composition and location of InSb nanophases.

4. Conclusions

The improvement of the multiple filling was observed in both the α and σ performance of the materials. Increasing the *In* content improved electrical performance of the material up to a limiting point of In concentration between $y = 0.1$ and $y = 0.2$. InSb and Yb₂O₃ nanophases are observed in the multi-filled systems and could be contributing to electrical performance enhancement of these materials. The sustainability of the *ZT* over a broad temperature range allows for more applications of these materials within the temperature range of 300–800 K. It appears the limit for *ZT* in the Ce_{0.1}In_{0.0.5}Yb_{0.2}Co₄Sb₁₂ sample has not been reached with an almost continual linear increase in *ZT* even at higher temperatures above 800 K. A state of the art maximum *ZT* of 1.4 at about 820 K was

found in the multiple filled $\text{Ce}_{0.1}\text{In}_{0.05}\text{Yb}_{0.2}\text{Co}_4\text{Sb}_{12}$. Furthermore, the ZT is still increasing at the highest measured temperature without any further contribution of the minority carriers.

Acknowledgments

We would like to acknowledge financial support acknowledge from a DOE/EPSCoR Implementation Grant (#DE-FG02-04ER-46139), and in addition, by the SC EPSCoR Office/Clemson University cost sharing. Also, thanks to recent support from a DOE subcontract to Nanosonic Inc.: E-4317: “Nanoscale Approach to High Performance Thermoelectric Composites.” Jian He would like to acknowledge financial support from NSF DMR-1307740.

Conflicts of Interest

The authors declare no conflict of interest.

References

1. Slack, G.A. *CRC Handbook of Thermoelectrics*; Rowe, D.M., Ed.; CRC Press: Boca Raton, FL, USA, 1995.
2. Klein, C.; Hurlbut, C.S., Jr. *Manual of Mineralogy*, 20th ed.; John Wiley: New York, NY, USA, 1985.
3. Nolas, G.S.; Slack, G.S.; Morelli, D.T.; Tritt, T.M.; Ehrlich, A.C. The effect of rare-earth filling on the lattice thermal conductivity of skutterudites. *J. Appl. Phys.* **1996**, *79*, 4002.
4. Zhao, X.Y.; Shi, X.; Chen, L.D.; Zhang, W.Q.; Zhang, W.B.; Pei, Y.Z. Synthesis and thermoelectric properties of Sr-filled skutterudite $\text{Sr}_y\text{Co}_4\text{Sb}_{12}$. *J. Appl. Phys.* **2006**, *99*, 053711.
5. Nolas, G.S.; Takizawa, H.; Endo, T.; Sellin, H.; Johnson, D.C. Thermoelectric properties of Sn-filled skutterudite. *Appl. Phys. Lett.* **2000**, *77*, 52.
6. Kuznetsov, V.L.; Kuznetsova, L.A.; Rowe, D.M. Effect of partial void filling on the transport properties of $\text{Nd}_x\text{Co}_4\text{Sb}_{12}$ skutterudites. *J. Phys.* **2003**, *15*, 5035–5048.
7. Zhang, J.; Xu, B.; Wang, L.M.; Yu, D.; Yang, J.; Yu, F.; Liu, Z.; He, J.; Wen, B.; Tian, Y. High-pressure synthesis of phonon-glass electron-crystal featured thermoelectric $\text{Li}_x\text{Co}_4\text{Sb}_{12}$. *Acta Mater.* **2012**, *60*, 1246–1251.
8. Nolas, G.S.; Cohn, J.L.; Slack, G.S. Effect of partial void filling on the lattice thermal conductivity of skutterudites. *Phys. Rev. B* **1998**, *58*, 164.
9. Lamberton, G.A., Jr.; Bhattacharya, S.; Littleton IV, R.T.; Kaeser, M.A.; Tedstrom, R.H.; Tritt, T.M. High figure of merit in Eu-filled CoSb_3 -based skutterudites. *Appl. Phys. Lett.* **2002**, *80*, 598.
10. Tritt, T.M. *Thermal Conductivity: Theory, Properties, and Applications*; Springer: New York, NY, USA, 2004.
11. Bai, S.Q.; Pei, Y.Z.; Chen, L.D.; Zhang, W.Q.; Zhao, X.Y.; Yang, J. Enhanced thermoelectric performance of dual-element-filled skutterudites $\text{Ba}_x\text{Ce}_y\text{Co}_4\text{Sb}_{12}$. *Acta Mater.* **2009**, *57*, 3135–3139.

12. Ballikaya, S.; Wang, G.; Sun, K.; Uher, C. Thermoelectric Properties of Triple-Filled $\text{Ba}_x\text{Yb}_y\text{In}_z\text{Co}_4\text{Sb}_{12}$. *J. Electron. Mater.* **2010**, *40*, 570–576.
13. Graff, J.W.; Zhu, S.; Holgate, T.; Peng, J.; He, J.; Tritt, T.M. High-Temperature Thermoelectric Properties of $\text{Co}_4\text{Sb}_{12}$ -Based Skutterdites with Multiple Filler Atoms: $\text{Ce}_{0.1}\text{In}_x\text{Yb}_y\text{Co}_4\text{Sb}_{12}$. *J. Electron. Mater.* **2011**, *40*, 696–701.
14. Morelli, D.T.; Meisner, G.P.; Chen, B.; Hu, S.; Uher, C. Cerium filling and doping of cobalt triantimonide. *Phys. Rev. B* **1997**, *56*, 7376.
15. Peng, J.; He, J.; Alboni, P.N.; Tritt, T.M. Synthesis and Thermoelectric Properties of the Double-Filled Skutterudite $\text{Yb}_{0.2}\text{In}_y\text{Co}_4\text{Sb}_{12}$. *J. Electron. Mater.* **2009**, *38*, 981–984.
16. Salvador, J.R.; Yang, J.; Wang, H.; Shi, X. Double-filled skutterudites of the type $\text{Yb}_x\text{Ca}_y\text{Co}_4\text{Sb}_{12}$: Synthesis and properties. *J. Appl. Phys.* **2010**, *107*, 043705.
17. Shi, X.; Kong, H.; Li, C.P.; Uher, C.; Yang, J.; Salvador, J.R.; Wang, H.; Chen, L.; Zhang, W. Low thermal conductivity and high thermoelectric figure of merit in *n*-type $\text{Ba}_x\text{Yb}_y\text{Co}_4\text{Sb}_{12}$. *Appl. Phys. Lett.* **2008**, *92*, 182101.
18. Shi, X.; Yang, J.; Salvador, J.R.; Chi, M.; Cho, J.Y.; Wang, H.; Bai, S.; Yang, J.; Zhang, W.; Chen, L. Multiple-Filled Skutterudites: High Thermoelectric Figure of Merit through Separately Optimizing Electrical and Thermal Transports. *J. Am. Chem. Soc.* **2011**, *133*, 7837–7846.
19. Zhang, L.; Grytsiv, A.; Rogl, P.; Bauer, E.; Zehetbauer, M. High thermoelectric performance of triple-filled *n*-type skutterudites $(\text{Sr},\text{Ba},\text{Yb})_y\text{Co}_4\text{Sb}_{12}$. *J. Phys. D* **2009**, *42*, 225405–225413.
20. He, T.; Chen, J.; Rosenfeld, D.; Subramanian, M.A. Thermoelectric Properties of Indium-Filled Skutterudites. *Chem. Mater.* **2006**, *18*, 759–762.
21. Peng, J.Y.; Alboni, P.N.; He, J.; Zhang, B.; Su, Z.; Holgate, T.; Gothard, N.; Tritt, T.M. Thermoelectric properties of (In,Yb) double-filled CoSb_3 skutterudite. *J. Appl. Phys.* **2008**, *104*, 053710.
22. Li, H.; Tang, X.F.; Zhang, Q.; Uher, C. High performance $\text{In}_x\text{Ce}_y\text{Co}_4\text{Sb}_{12}$ thermoelectric materials with in situ forming nanostructured InSb phase. *Appl. Phys. Lett.* **2009**, *94*, 102114.
23. Qi, W.H.; Wang, M.P. Size effect on the cohesive energy of nanoparticle. *J. Mat. Sci. Lett.* **2002**, *21*, 1743.
24. Nanda, K.K.; Sahu, S.N.; Behera, S.N. Liquid-drop model for the size-dependent melting of low-dimensional systems. *Phys. Rev. A* **2002**, *66*, 013208.
25. Frenken, J.W.M.; van der Veen, J.F. Observation of Surface Melting. *Phys. Rev. Lett.* **1985**, *54*, 134.
26. Pope, A.L.; Littleton, R.T., IV; Tritt, T.M. Apparatus for the rapid measurement of electrical transport properties for both “needle-like” and bulk materials. *Rev. Sci. Instru.* **2001**, *72*, 3129.
27. Pope, A.L.; Zawilski, B.; Tritt, T.M. Description of removable sample mount apparatus for rapid thermal conductivity measurement. *Cryogenics* **2001**, *41*, 725–731.